

05,09,10

# Impurity Reverse Magnetoelectric Effect in a Semiconductor Quantum Well

© A.B. Grunin

Federal State Budgetary Educational Institution of Higher Education  
„Penza State University“,  
Penza, Russia

E-mail: grunin.sky@yandex.ru

Received November 22, 2025

Revised February 21, 2026

Accepted February 22, 2026

A theoretical study is presented of the impurity reverse magnetoelectric effect (ME) in a semiconductor quantum well (QW) with a parabolic confinement potential containing a  $D^{(-)}$  center (negative ion donor). Within the framework of the zero-radius potential model, in the effective mass approximation, a dispersion equation is obtained that determines the binding energy of the impurity state, analytical expressions for the impurity wave function and the dipole magnetic moment induced by an electric field for the impurity electron in the QW. Numerical analysis revealed an asymmetry in the field dependence of the dipole magnetic moment relative to the impurity coordinate due to a violation of the space-time symmetry of the nanostructure. For the positions of the  $D^{(-)}$  center shifted relative to the plane of symmetry of the QW in the direction opposite to the electric field strength, the field dependence of the dipole magnetic moment is non-monotonic with a maximum in the paramagnetic region and a transition to the diamagnetic one. The possibility of controlling the considered ME using both fields and deliberate selective alloying is shown.

**Keywords:** toroidal moment, asymmetric nanostructures, donor impurities, Green's function method, effective mass method, zero-radius potential model.

DOI: 10.61011/PSS.2026.02.63382.330-25

## 1. Introduction

The interest in the systems with a disturbed spatiotemporal symmetry has been steadily rising after I.E. Dzyaloshinski [1] in 1959 predicted the existence of the magnetoelectric effect (ME) in magnetic crystals with a point group with absent time inversion  $t \rightarrow -t$ , and after D.N. Astrov in 1960 discovered the inverse ME [2], and later G.T. Rado and V.J. Folen discovered direct ME [3] in the crystals of the antiferromagnetic  $\text{Cr}_2\text{O}_3$ .

It is known that disturbed macroscopic symmetry arises because of a certain type of ordering with a characteristic order parameter: in the ferroelectric state — polar vector of electric polarization  $\mathbf{P}$ , in the ferromagnetic phase — axial vector of magnetization (or magnetic moment)  $\mathbf{P}_m$ , in the toroidal state —  $t$ -odd polar vector of the toroidal moment  $\mathbf{T}$ ,  $t$ -even axial vector  $\mathbf{G}$  characterizing the ordering of spin currents in the system.

The coexistence of electric and magnetic ordering made it possible to synthesize [4,5] and investigate ferromagnetic compounds [6–8]. In [9], the introduction of a toroidal order parameter of both spin and orbital nature into the condensed matter physics was theoretically justified. The toroidal moment was detected in a strong magnetic field in  $\text{Cr}_2\text{O}_3$  [10], as well as in a ferromagnetic compound  $\text{Ga}_{2-x}\text{Fe}_x\text{O}_3$  [11], and also in  $\text{LiCoPO}_4$  toroidal domains were found by the optical method of second harmonic generation [12].

A new subclass of magnetoelectric materials, in a broader sense, a subclass of antiferromagnetic materials — materials with a toroidal arrangement or toroids are characterized by significantly high values of the magnetoelectric coefficient [13,14]. At the same time, ME manifests itself more strongly in nanostructures than in bulk materials, which is due to the difference in the characteristic spatial scales of changes in potential energy and wave functions in these systems [13]. In orbital toroids, the ME can be large compared to spin toroids due to the smallness of the spin-orbit interaction. The presence in the system of a toroidal moment vector  $\mathbf{T}$  with a symmetry similar to that of the quasi-pulse  $\mathbf{p} = \hbar\mathbf{k}$  of the charge carriers, where  $\mathbf{k}$  is a quasi-wave vector, leads to an asymmetry of the spectrum of elementary excitations along the quasi-pulse  $E(\mathbf{k}) \propto \mathbf{T} \cdot \mathbf{k}$  [13]. In [15], a strong non-relativistic orbital longitudinal and transverse ME was studied in tunnel-coupled asymmetric quantum wells (AQW) in a magnetic field longitudinal relative to their plane  $\mathbf{B}$ , simulating a disturbed temporal symmetry. The authors noted the nonlinear nature of polarization vector  $\mathbf{P} \propto [\mathbf{B}, \mathbf{T}] = (\mathbf{B}, \mathbf{I}) \cdot \mathbf{B} - \mathbf{I} \cdot \mathbf{B}^2$  versus magnetic induction vector curve, while  $\mathbf{T} \propto [\mathbf{B}, \mathbf{I}]$ , where  $\mathbf{i}$  was a polar vector directed along AQW growth axis.

Also, the study [15] shows high sensitivity of ME to the degree of the system disequilibrium, especially in the case of doped asymmetric heterostructures [13], when the effect is compensated by free charge carriers. It should be

stressed that a large number of works are devoted to the theoretical and experimental study of direct ME as opposed to inverse ME, the latter of which has its essential practical application in the design of resonators, microwave filters, microwave attenuators controlled by an electric field, as well as in promising magnetic memory elements with electrical recording and reading information [19,20].

These reasons make it relevant to study the inverse ME for the charge carriers localized on impurity centers in asymmetric nanostructures with the disturbed spatiotemporal symmetry.

The purpose of this work is to theoretically study the inverse ME caused by  $n$ -type impurity with an additional electron ( $D^{(-)}$  center) in an asymmetric semiconductor quantum well (QW) with a disturbed spatiotemporal symmetry, i.e., to study the doped inverse ME. The spatial asymmetry is caused by electric field and the temporal one is simulated by magnetic field. The effect is considered at low temperatures  $T$ , when the average thermal energy is  $k_B T \ll |E_i|$ , where  $k_B$  is the Boltzmann constant,  $|E_i|$  is the ionization energy of the impurity center.

## 2. Theoretical background

Let's place a semiconductor QW with a parabolic confinement potential in a longitudinal (with respect to its axis of dimensional quantization) constant electric field with a strength of  $\mathbf{E}$  and a transverse (lying in the QW plane) constant magnetic field with induction  $\mathbf{B}$ .

To theoretically describe the single-electron states in semiconductor nanostructures, the „rigid-wall“ [21] model is often used, i.e., the confinement potential is selected as a potential well of the appropriate dimension with infinitely high walls. In this case, although the bottom of the potential well is flat, the solution of Schrodinger equation is irregular: the electron density in the QW is unevenly distributed. The approximation of QW by a rectangular potential profile in the absence of local electroneutrality leads to an internal contradiction of the model: the type of single-electron wave functions stands for an inhomogeneous distribution of charge (and potential), while the well bottom remains flat. As seen from the analysis of the self-consistency numerical solution of Poisson equation and Schrodinger equation for the QWs [22], the confinement potential is almost a parabolic potential itself, but with the lower part cut off [22,23]. This form of potential is quite close to the parabolic one, which makes it possible to consider the latter quite realistic [24].

Let's assume that QW symmetry plane coincides with  $xy$  plane, magnetic induction vector  $\mathbf{B}$  is directed in this plane along  $y$  axis, and  $z$  axis is directed along the QW dimensional quantization. In the asymmetric calibration, the vector potential  $\mathbf{A}$  has the form

$$\mathbf{A} = B_y \cdot z \cdot \mathbf{e}_x, \quad (1)$$

where  $\mathbf{B}(0, B_y, 0)$ ;  $\mathbf{e}_x$  — unit vectors along  $x$  axis.

Schrödinger equation for the motion of an electron in the QW conduction band (CB) in the considered electric and magnetic fields is written as

$$\hat{H}\Psi_{n,k_x,k_y}(x, y, z) = E_n(k_x, k_y)\Psi_{n,k_x,k_y}(x, y, z), \quad (2)$$

here the Hamiltonian is equal

$$\hat{H} = -\frac{\hbar^2}{2m^*} \nabla^2 - i\hbar\omega_c \cdot z \frac{\partial}{\partial x} + \frac{m^* \Omega^2 z^2}{2} + e \cdot E_z \cdot z, \quad (3)$$

$\nabla^2$  — Laplace operator;  $\omega_c = eB_y/m^*$  — cyclotron frequency;  $\mathbf{E} = (0, 0, E_z)$ ;  $e$  — elementary electrical charge,  $m^*$  — effective mass of the electron;  $\Omega = \sqrt{\omega_0^2 + \omega_c^2}$  — hybrid frequency,  $\omega_0$  — frequency of the parabolic holding potential of QW

$$V(z) = \frac{m^* \omega_0^2 z^2}{2}, \quad (4)$$

with the amplitude  $U_0 = m^* \omega_0^2 L^2 / 2$ , where  $2L$  — width of QW.

Since the QW holding potential must have a finite depth, in the chosen oscillatory model of the confinement potential, the potential amplitude  $U_0$  is an empirical parameter. Let's assume that  $U_0$  meets the condition [25]

$$\frac{U_0}{\hbar\omega_0} \ll 1. \quad (5)$$

It is known that the solution of the stationary Schrödinger equation (2) with a Hamiltonian (3) without an electric field has been considered in a number of papers [26,27].

Then, the eigen wave functions and the electron energy spectrum for Hamiltonian (3) taking into account (5) can be written as

$$\Psi_{n,k_x,k_y}(x, y, z) = (2^n n! \sqrt{\pi} a_\Omega L_x L_y)^{-1/2} \cdot H_n \left( \frac{z - z_0(k_x)}{a_\Omega} \right) \times \exp \left( -\frac{(z - z_0(k_x))^2}{2 \cdot a_\Omega^2} \right) \exp(ik_x x + ik_y y), \quad (6)$$

$$E_n(k_x, k_y) = \hbar\Omega \left( n + \frac{1}{2} \right) + \frac{\hbar^2(k_x^2 + k_y^2)}{2m^*} - \frac{m^* \Omega^2 z_0^2(k_x)}{2}, \quad (7)$$

where  $n = 0, 1, 2, \dots$ ;  $H_n(z)$  — Hermitian polynomials;  $a_\Omega = \sqrt{\hbar/(m^* \Omega)}$  — hybrid length;  $L_x, L_y$  — linear dimensions of QW in  $xy$  plane;  $k_x, k_y$  — projections of the quasi-wave vector  $\mathbf{k}$  of electron;

$$z_0(k_x) = -\frac{e \cdot E_z + \hbar \cdot \omega_c k_x}{m^* \Omega^2}, \quad (8)$$

the coordinate of the hybrid oscillator center in the electromagnetic field, which determines the anisotropy of the electron energy

$$E_n(k_x, k_y) \neq E_n(-k_x, k_y). \quad (9)$$

Local electronic states induced by defects lying inside QW have been intensively studied in [28,29] due to the development of  $\delta$ -doping technology. In theoretical studies on the local  $D^{(-)}$  states in a semiconductor QW in the absence of [21,30] and in the presence of [25] magnetic field (longitudinal with respect to the QW growth axis) a zero-radius potential model for the defect potential was used. It is known [30] that zero-radius potential model well describes both  $D^{(-)}$  states and the states of the negative hydrogen ion  $H^-$ , i.e., because these states are small (their binding energy is about 5% of Bohr energy) and, consequently, the corresponding localization radius of the confined electron is significantly larger than the effective radius of the potential, i.e., the latter is determined by the Bohr radius. This model allows obtaining an analytical solution for the wave function, as well as the dispersion equation of an electron localized at  $D^{(0)}$  center.

Let's  $D^{(-)}$  center be localized in point  $\mathbf{R}_a = (x_a, y_a, z_a)$ . The impurity potential is described within the zero-radius potential model  $\hat{V}_\delta(\mathbf{r}, \mathbf{R}_a)$  with power  $\gamma = 2\pi\hbar^2/(\alpha m^*)$ :

$$\hat{V}_\delta(\mathbf{r}, \mathbf{R}_a) = \gamma\delta(\mathbf{r} - \mathbf{R}_a)(1 + (\mathbf{r} - \mathbf{R}_a)\nabla_r), \quad (10)$$

where  $\alpha$  is determined by the energy  $E_i = -\hbar^2\alpha^2/(2m^*)$  of the bound state of the same  $D^{(-)}$  center in the bulk material;  $\delta(x)$  — Dirac delta function;  $\nabla_r$  — the gradient operator in the coordinate space. Taking into account expression (10), Schrödinger equation for an electron localized at  $D^{(0)}$ -center in the QW in electric and magnetic fields will be written as

$$(\hat{H} + \hat{V}_\delta(\mathbf{r}, \mathbf{R}_a))\Psi_\lambda^{(QWell)}(\mathbf{r}, \mathbf{R}_a) = E_\lambda \cdot \Psi_\lambda^{(QWell)}(\mathbf{r}, \mathbf{R}_a), \quad (11)$$

here,  $E_\lambda = -\hbar^2\lambda^2/(2m^*)$  — eigen values of Hamiltonian in (11).

$$\begin{aligned} G(\mathbf{r}, \mathbf{R}_a; E_\lambda) = & -\frac{\sqrt{\pi}}{a_\Omega a_d^2 E_d} \left( \int_0^{+\infty} dt \cdot t^{-1/2} \exp(-\varepsilon_s t) \exp\left(-\frac{(y-y_a)^2}{4a_d^2 t}\right) \right) \\ & \times \left\{ [f(\Omega, t)]^{-1/2} \exp\left[\frac{|\Delta\varepsilon_{St}| \cdot t}{f(\Omega, t)} \left( \left(\frac{\omega_c}{\Omega}\right)^2 \cdot r(\Omega, t) - \left(\frac{a_\Omega}{a_d}\right)^2 \text{th}(u) \right)\right] (1 - \exp[-4u])^{-1/2} \exp\left(-\frac{(y-y_a)^2}{4a_d^2 t}\right) \right. \\ & \times \exp\left[-\frac{(z_a^2 + z^2)}{2a_\Omega^2} \frac{g(\Omega, t)}{f(\Omega, t)}\right] \exp\left(\frac{z_a z \cdot h(\Omega, t)}{2a_d^2 \cdot f(\Omega, t)}\right) \exp\left(-\frac{(z+z_a) \sqrt{|\Delta\varepsilon_{St}|} \text{th}(u)}{a_d \cdot f(\Omega, t)}\right) \exp\left\{-\frac{i \frac{\omega_c}{\Omega} (x-x_a)(z+z_a) \text{th}(u)}{2a_\Omega^2 f(\Omega, t)}\right\} \\ & \times \exp\left(-\frac{(x-x_a)^2}{4a_d^2 f(\Omega, t)} + \frac{i \frac{\omega_c}{\Omega} (x-x_a) \sqrt{|\Delta\varepsilon_{St}|} r(\Omega, t)}{a_d \cdot f(\Omega, t)}\right) - \frac{a_\Omega}{2a_d t} \exp\left[-\frac{(\mathbf{r}-\mathbf{R}_a)^2}{4a_d^2 t}\right] \left. \right\} + \sqrt{\pi} a_\Omega \frac{\exp\{-\sqrt{\varepsilon_s} \cdot \frac{|\mathbf{r}-\mathbf{R}_a|}{a_d}\}}{|\mathbf{r}-\mathbf{R}_a|}, \quad (14) \end{aligned}$$

where  $i^2 = -1$ .

Following the well-known standard procedure (e.g., [31]), the equation (11) is solved using Green's function  $G(\mathbf{r}, \mathbf{R}_a; E_\lambda)$ , which differs by a constant factor from the wave function of  $D^{(-)}$  state:

$$\Psi_\lambda^{(QWell)}(\mathbf{r}, \mathbf{R}_a) = -C_\lambda^{(QWell)} a_\Omega a_d^2 E_d G(\mathbf{r}, \mathbf{R}_a; E_\lambda), \quad (12)$$

here, the normalization factor  $C_\lambda^{(QWell)}$  is equal

$$\begin{aligned} C_\lambda^{(QWell)} = & \left[ \frac{\partial G(\mathbf{R}_a, \mathbf{R}_a; E_\lambda)}{\partial \varepsilon_s} \right]^{-1/2} = a_\Omega^{-1/2} a_d^{-1} \pi^{-1/4} \\ & \times \int_0^\infty dt \cdot t^{1/2} \exp(-\varepsilon_s t) [f(\Omega, t)]^{-1/2} \cdot (1 - \exp[-4u])^{-1/2} \\ & \times \exp\left[\frac{|\Delta\varepsilon_{St}| \cdot t}{f(\Omega, t)} \left( \left(\frac{\omega_c}{\Omega}\right)^2 \cdot r(\Omega, t) - \left(\frac{a_\Omega}{a_d}\right)^2 \text{th}(u) \right)\right] \\ & \times \exp\left[-\frac{z_a^2}{a_\Omega^2 f(\Omega, t)} \left( g(\Omega, t) - \frac{a_\Omega^2}{2a_d^2} h(\Omega, t) \right)\right] \\ & \times \exp\left(-\frac{2z_a \sqrt{|\Delta\varepsilon_{St}|} t \cdot \text{th}(u)}{a_d \cdot f(\Omega, t)}\right)^{-1/2}, \quad (13) \end{aligned}$$

$E_d = \hbar^2/(2m^* a_d^2)$ ,  $a_d = 4\pi\varepsilon_0 \hbar^2/(m^* e^2)$  — effective Bohr energy and Bohr radius, respectively;  $\varepsilon$  — static dielectric permittivity of matter,  $\varepsilon_0$  — electric constant;  $\varepsilon_s = (E_0(0, 0) - E_\lambda)/E_d$  — doped electron bond energy counted from the energy of the ground state  $E_0(0, 0)$  of electron in QW (7) at  $n=0$ ,  $k_x=0$  and  $k_y=0$  in the units of effective Bohr energy;  $\Delta\varepsilon_{St} = -(eE_z)^2/(2m^* \Omega^2 E_d)$  — Stark energy levels shift;  $u = (a_d/a_\Omega)^2 t$ ;  $f(\Omega, t) = (\omega_0/\Omega)^2 t + (\omega_c/\Omega)^2 (a_\Omega/a_d)^2 \text{th}(u)$ ,  $r(\Omega, t) = t - (a_\Omega/a_d)^2 \text{th}(u)$ ,  $g(\Omega, t) = (\omega_0/\Omega)^2 t \text{cth}[2u] + (\omega_c/\Omega)^2 (a_\Omega/a_d)^2 / 2$ ,  $h(\Omega, t) = 2(\omega_0/\Omega)^2 (a_d/a_\Omega)^2 \frac{t}{\text{sh}(2u)} + (\omega_c/\Omega)^2$ ,  $\text{th}(x)$ ,  $\text{cth}(x)$ ,  $\text{sh}(x)$  — hyperbolic tangent, cotangent, and sine, respectively; one-electron Green's function  $G(\mathbf{r}, \mathbf{R}_a; E_\lambda)$  in the effective mass approximation with an indicated divergent part [31]:

According to a well-known method [31], we write down an explicit form of the dispersion equation that determines the bond energy of  $D^{(-)}$  state versus parameters of a QW located in a longitudinal constant electric field with a strength  $\mathbf{E}$  and a transverse permanent magnetic field with induction  $\mathbf{B}$ , the positions of the impurity center:

$$\begin{aligned} \alpha = & 4\pi^{3/2} a_{\Omega}^{-1} \left\{ \int_0^{+\infty} dt \cdot t^{-1/2} \exp(-\varepsilon_s t) \right. \\ & \times \left[ [f(\Omega, t)]^{-1/2} \cdot (1 - \exp[-4u])^{-1/2} \right. \\ & \times \exp \left[ - \left( \left( \frac{z_a}{a_{\Omega}} \right)^2 + 2 \frac{z_a}{a_d} \sqrt{|\Delta\varepsilon_{St}|} + \left( \frac{a_{\Omega}}{a_d} \right)^2 |\Delta\varepsilon_{St}| \right) \text{th}(u) \right] \\ & \times \exp \left[ \left( \frac{\omega_c}{\Omega} \right)^2 \frac{\left( -\frac{z_a}{a_d} \text{th}(u) + \sqrt{|\Delta\varepsilon_{St}|} \cdot r(\Omega, t) \right)^2}{f(\Omega, t)} \right] - \frac{a_{\Omega}}{2a_d t} \right] \\ & \left. - \sqrt{\pi} \frac{a_{\Omega}}{a_d} \sqrt{\varepsilon_s} \right\}. \quad (15) \end{aligned}$$

Let's find the average projection of the dipole magnetic moment  $\langle p_y^{(m)} \rangle(\mathbf{E}, \mathbf{B}, z_a)$  of an impurity electron using the expression for the wave function of the impurity state (12), taking into account (13) and (14)

$$\begin{aligned} \langle p_y^{(m)} \rangle(\mathbf{E}, \mathbf{B}, z_a) = & \frac{ie\hbar}{2m^*} \int_{-\infty}^{+\infty} \int_{-\infty}^{+\infty} \int_{-\infty}^{+\infty} d^3\mathbf{r} \left( \Psi_{\lambda}^{(\text{QWell})}(\mathbf{r}, \mathbf{R}_a) \right)^* \\ & \times \left( z \frac{\partial}{\partial x} - x \frac{\partial}{\partial z} \right) \Psi_{\lambda}^{(\text{QWell})}(\mathbf{r}, \mathbf{R}_a). \quad (16) \end{aligned}$$

The additional dipole magnetic moment  $\langle \Delta p_y^{(m)} \rangle(\mathbf{E}, \mathbf{B}, z_a)$  of an electron at  $D^{(0)}$ -center, caused by the joint action of mutually perpendicular electric and magnetic fields, is determined by the expression

$$\langle \Delta p_y^{(m)} \rangle(\mathbf{E}, \mathbf{B}, z_a) = \langle p_y^{(m)} \rangle(\mathbf{E}, \mathbf{B}, z_a) - \langle p_y^{(m)} \rangle(0, \mathbf{B}, z_a). \quad (17)$$

The analytical calculation in the formula (16) of integrals in coordinate variables is performed using well-known Poisson type integrals [32]:

$$\begin{aligned} \int_{-\infty}^{+\infty} dx x^n \exp(-px^2 + 2qx) = & n! \left( \frac{q}{p} \right)^n \sqrt{\frac{\pi}{p}} \\ & \times \exp\left( \frac{q^2}{p} \right) \sum_{k=0}^{[n/2]} \frac{1}{(n-2k)!k!} \left( \frac{p}{4q^2} \right)^k, \quad (18) \end{aligned}$$

here  $p > 0$  and  $[n/2]$  — integral part of the number  $n/2$ .

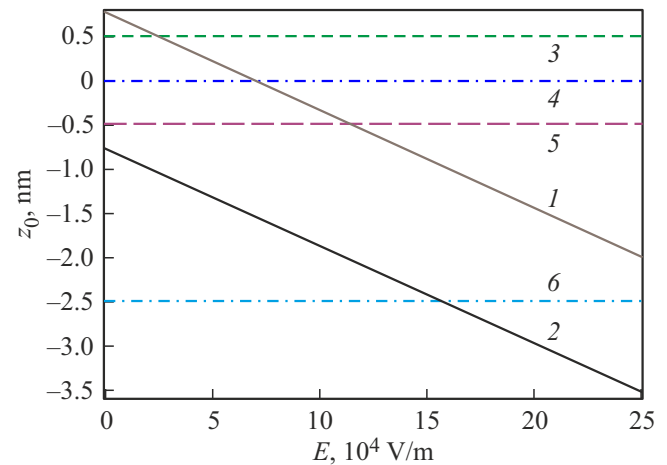
The internal double integral in (16) with respect to the variables  $t$  and  $t_1$  (varies within the same limits as  $t$  in expression (14)) contained in integral representations

of complex-conjugate wave functions  $\Psi_{\lambda}^{(\text{QWell})}(\mathbf{r}, \mathbf{R}_a)$  and  $(\Psi_{\lambda}^{(\text{QWell})}(\mathbf{r}, \mathbf{R}_a))^*$  of the dopes state, is found by numerical integration using cubature formulae [33,34].

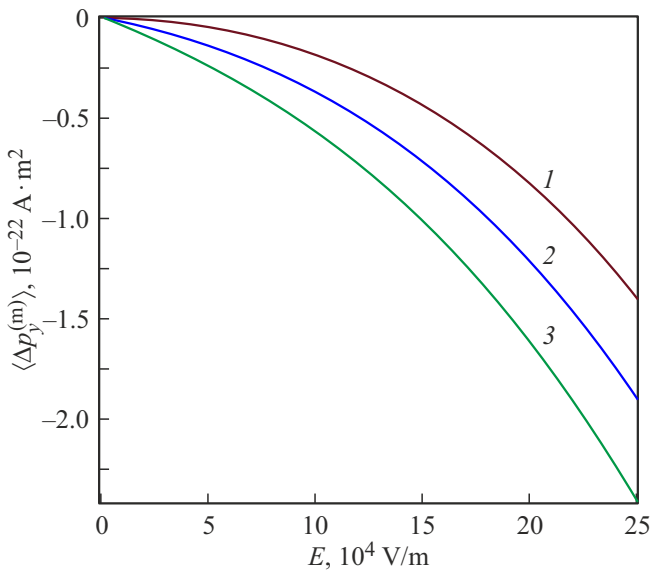
### 3. Discussion of findings

Figure 1 shows the dependence of the coordinate  $z_0(k_x, \mathbf{E}, \mathbf{B})$  of the hybrid oscillator's center on the electric field strength  $\mathbf{E}$  for two opposite projections  $k_x$  of the quasi-wave vector  $\mathbf{k}$  and a fixed value of the magnetic induction  $\mathbf{B}$ . That is, since for  $k_x < 0$  and  $k_x > 0$  the oscillator centers are spatially spaced apart, and the wave function of the impurity state is constructed from the wave functions of WQ CB states, then, the prevailing contribution into the state of  $D^{(-)}$  center will be provided by the states with such  $k_x$ , for which the oscillators' centers were close to position  $z_a$  of the impurity center, i.e.  $|z_a - z_0(k_x)| \ll a_{\Omega}$ . Therefore,  $z_a > 0$  (line 3),  $z_a = 0$  (line 4) a significant contribution is provided by the states with  $k_x < 0$  (line 1). For  $z_a < 0$  in Figure 1 with  $z_a^{(1)} > z_0(k_x > 0, \mathbf{E} = 0, \mathbf{B})$  as an example (line 5) we see the change of the prevailing contribution ensured by the states with  $k_x > 0$  (line 2) into the contribution of states with  $k_x < 0$  with the strength rise. If, without changing the electric field, the impurity center is moved opposite to the voltage vector  $E$  to the position  $z_a^{(2)} < z_0(k_x > 0, \mathbf{E} = 0, \mathbf{B})$  (line 6), there will be a transition from a greater contribution of states with  $k_x < 0$  to a prevailing contribution of states with  $k_x > 0$ .

The considered mechanism of changing the wave function of the impurity state depending on the coordinate of  $z_a$   $D^{(0)}$ -center and the electric field strength determines the de-



**Figure 1.** Coordinate of the oscillator's center  $z_0(k_x)$  in a InSb based QW with parameters  $L = 72$  nm,  $U_0 = 0.2$  eV versus electric field strength in the magnetic field with induction  $B = 1$  T for the two opposite projections of the quasi-wave vector  $\mathbf{k}$ : curve 1 —  $k_x < 0$ ; 2 —  $k_x > 0$ . The lines show position of  $D^{(0)}$ -center with various  $z_a$ : curve 3 —  $z_a > 0$ , 4 —  $z_a = 0$ ; 5 —  $z_0(k_x > 0, \mathbf{E} = 0, \mathbf{B}) < z_a < 0$ ; 6 —  $z_a < z_0(k_x > 0, \mathbf{E} = 0, \mathbf{B}) < 0$ .



**Figure 2.** The average value  $\langle \Delta p_y^{(m)} \rangle$  of the projection of the additional dipole magnetic moment of  $D^{(-)}$  center ( $|E_i| = 0.03 \text{ eV}$ ) in InSb QW ( $L = 72 \text{ nm}$ ,  $U_0 = 0.2 \text{ eV}$ ) versus electrical field strength  $E$  in the magnetic field with induction  $B = 1 \text{ T}$  for various coordinates  $z_a \geq 0$ : curve 1 —  $z_a = 0 \text{ nm}$ ; 2 —  $z_a = 0.5 \text{ nm}$ ; 3 —  $z_a = 1 \text{ nm}$ .

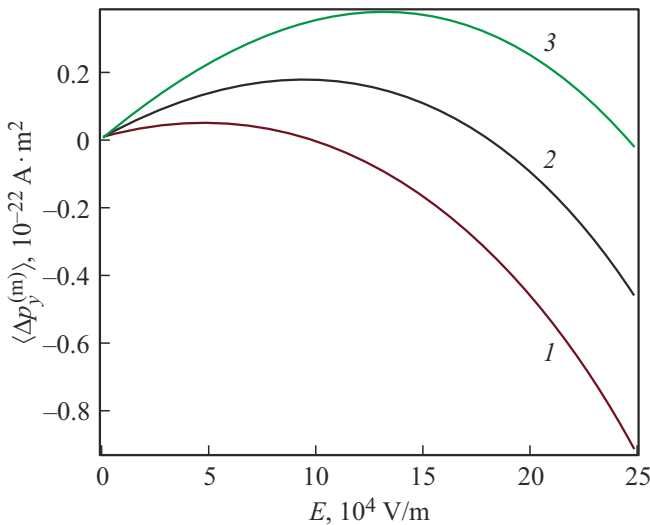


**Figure 3.** The average value  $\langle \Delta p_y^{(m)} \rangle$  of the projection of the additional dipole magnetic moment of  $D^{(-)}$  center ( $|E_i| = 0.03 \text{ eV}$ ) in InSb based QW ( $L = 72 \text{ nm}$ ,  $U_0 = 0.2 \text{ eV}$ ) versus electrical field strength  $E$  in the magnetic field with induction  $B = 1 \text{ T}$  for various coordinates  $z_a < 0$ : curve 1 —  $z_a = -0.5 \text{ nm}$ ; 2 —  $z_a = -1 \text{ nm}$ ; 3 —  $z_a = -1.5 \text{ nm}$ .

pendence of the average projection of the additional dipole magnetic moment  $\langle \Delta p_y^{(m)} \rangle(\mathbf{E}, \mathbf{B}, z_a)$  of the impurity electron onto magnetic induction direction  $\mathbf{B}$  on the electrical field. Thus, Figure 2 illustrates  $\langle \Delta p_y^{(m)} \rangle$  versus electrical field strength  $\mathbf{E}$  for  $z_a \geq 0$ . The curve 1 shows that in weak electric fields, the additional dipole magnetic moment is

directed opposite to the magnetic induction vector  $\mathbf{B}$  and in absolute value  $\propto E^2$ . With the growth of coordinate  $z_a$  additional magnetic moment also rises (see the curves 2 and 3 Figure 2). Figure 3 illustrates  $\langle \Delta p_y^{(m)} \rangle$  versus strength of electric field  $\mathbf{E}$  for  $z_a < 0$ . In accordance with the explanation to Figure 1 and the above, the initial section of the curve 1 in Figure 3 corresponds to a small contribution of states with  $k_x > 0$ , followed by a predominance of states with  $k_x < 0$ . As the absolute value of  $|z_a|$  rises, there occurs a slight (curve 2), and then a more noticeable (curve 3) deviation from the monotonic dependence with a characteristic maximum in the region of  $\langle \Delta p_y^{(m)} \rangle > 0$  and a change in the direction of the dipole magnetic moment vector  $\langle \Delta \mathbf{p}^{(m)} \rangle$  to the opposite with a further increase in the absolute value of the projection  $|\langle \Delta p_y^{(m)} \rangle| \propto E^2$  in weak fields (curves 2 and 3). As seen from the numerical analysis with the rise of magnetic induction  $B$  the point of maximum  $E_{\text{max}}$  and electrical field strength  $E_0$  at which the additional dipole magnetic moment  $\langle \Delta p_y^{(m)} \rangle = 0$  do not change and maximal value grows — is equal  $\langle \Delta p_y^{(m)} \rangle(E_{\text{max}}) \propto B$ .

Figure 4 shows the relative change in the average value of the projection of the additional dipole magnetic moment  $\delta \langle p_y^{(m)} \rangle$  versus coordinate of the impurity center  $z_a$ . When the  $D^{(0)}$  center is shifted in the direction of the electric field strength  $\mathbf{E}$  from the values  $z_a < 0$  to  $z_a > 0$ , the projection  $\delta \langle p_y^{(m)} \rangle$  decreases linearly to zero and increases linearly when changing the sign. In region  $z_a < 0$  the dipole magnetic moment gets a paramagnetic admixture, and in  $z_a \geq 0$  — a diamagnetic admixture (see the curve 1). As the electric field strength grows, the diamagnetic region shifts towards negative values  $z_a$ , and the values of the diamagnetic and paramagnetic corrections themselves increase (see curve 2).

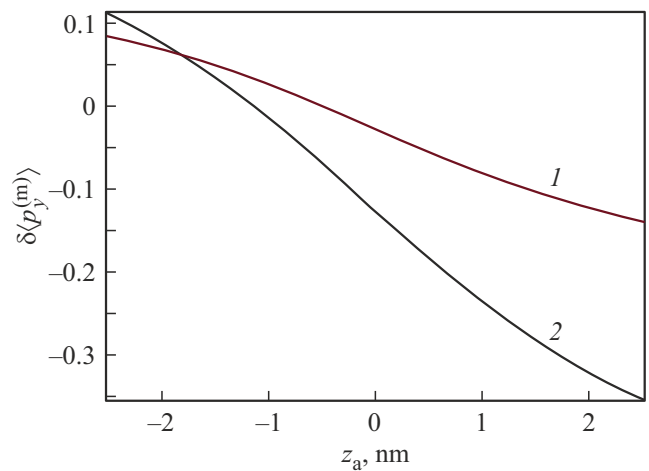


**Figure 4.** The relative change of the average value  $\delta \langle p_y^{(m)} \rangle$  of the projection of additional dipole magnetic moment of  $D^{(-)}$  center ( $|E_i| = 0.03 \text{ eV}$ ) in InSb QW ( $L = 72 \text{ nm}$ ,  $U_0 = 0.2 \text{ eV}$ ) versus the coordinate of the impurity center  $z_a$  in magnetic field  $B = 1 \text{ T}$  for various electrical field strengths: curve 1 —  $E = 1 \cdot 10^5 \text{ V/m}$ ; 2 —  $E = 2 \cdot 10^5 \text{ V/m}$ .

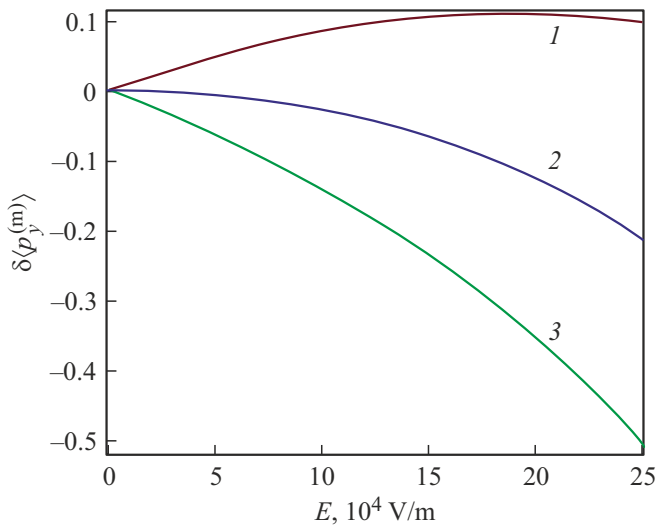


**Figure 5.** The relative change of the average value  $\delta\langle p_y^{(m)} \rangle$  of the projection of additional dipole magnetic moment of  $D^{(-)}$  center ( $|E_i| = 0.03$  eV) in InSb QW ( $L = 72$  nm,  $U_0 = 0.2$  eV) versus the electrical field strength  $E$  in the magnetic field with induction  $B = 1$  T for various positions of  $z_a$  impurity: 1 curve— $z_a = -2.5$  nm; 2 —  $z_a = 0$  nm; 3 —  $z_a = 2.5$  nm.

Figure 5 shows the relative change in the average value of the projection of the additional dipole magnetic moment  $\delta\langle p_y^{(m)} \rangle$  versus electrical field strength  $E$  and various positions of  $z_a$   $D^{(0)}$ -center. In weak electric fields, the considered dependence is quadratic (curves 1–3) with a characteristic maximum on curve 1 for  $z_a < 0$ . It should be noted that when  $D^{(0)}$ -center is shifted in the direction of the electric field, the magnitude of the relative change  $\delta\langle p_y^{(m)} \rangle$  increases (see curves 1–3), varying from approximately 10 to 50%.

Estimation of the magneto-electric coefficient (MEC)  $\alpha^{(ME)}$  by numerical analysis for a single QW containing  $D^{(-)}$  centers with a surface concentration of  $N_s \approx 10^{10}$  cm $^{-2}$  [28] in planes with the coordinate  $z_a$ , embedded by planar selective doping [28,35], gives the value  $\alpha^{(ME)} \sim 10^{-13} - 10^{-12}$  s  $\cdot$  m $^{-1}$  for the QW parameters, impurity center characteristics, and values of strength  $E \approx 10^5$  V/m, and magnetic induction  $B \approx 1$  T, which is close in order of magnitude to single-phase magnetoelectric materials at temperatures  $T \approx 10$  K [36]. MEC  $\alpha^{(ME)}$  calculated in [13] for an asymmetric non-doped heterostructure with three tunnel-connected QW at  $T = 5.8$  K and magnetic induction of  $B \approx 1$  T makes  $\sim 10^{-14} - 10^{-13}$  s  $\cdot$  m $^{-1}$ . This shows that the contribution of impurity states to ME is significant in these conditions.

## 4. Conclusion

A theoretical study of the impurity inverse ME in a QW with a parabolic confinement potential located in a constant longitudinal electric field relative to its axis of dimensional

quantization and a transverse magnetic field is carried out. In zero-radius potential model, a dispersion equation for  $D^{(-)}$  state is obtained in the effective mass approximation, which determines the dependence of the binding energy of an impurity electron on the parameters of  $D^{(0)}$  center, QW characteristics, and the electric and magnetic field strengths. Also, the Green's function method was applied to find the analytical expression for the wave function of  $D^{(-)}$  state, which is used to calculate the average projection of the additional dipole magnetic moment  $\Delta\langle p_y^{(m)} \rangle$  on the magnetic field direction. Numerical integration has demonstrated that the value  $\Delta\langle p_y^{(m)} \rangle$  in weak electric fields varies according to the quadratic law and significantly depends on the position of the impurity center. For  $D^{(0)}$  centers located in the plane of symmetry of QW or shifted relative to it in the direction of the electric field, the additional dipole magnetic moment is antiparallel to the magnetic induction vector. For  $D^{(0)}$  centers shifted relative to the QW symmetry plane opposite to the electric field strength, the dependence of the additional dipole magnetic moment on the electric field strength becomes nonmonotonic: the magnetoelectric correction  $\Delta\langle p_y^{(m)} \rangle$  is paramagnetic with a characteristic maximum at the initial section of the field dependence; then, decreasing and changing its sign, it becomes diamagnetic. The maximum in region  $\Delta\langle p_y^{(m)} \rangle > 0$  shifts towards large electric fields with increasing distance from the impurity to QW symmetry plane. Changing the impurity center position makes it possible to control both the value and the direction of the additional dipole magnetic moment of the impurity electron.

## Conflict of interest

The author declares no conflict of interest.

## References

- [1] I.E. Dzyaloshinskii. JETP **10**, 3, 628 (1960).
- [2] D.N. Astrov. JETP **11**, 3, 708 (1960).
- [3] G.T. Rado, V.J. Folen. Phys. Rev. Lett. **7**, 8, 310 (1961).
- [4] G.A. Smolensky, A.I. Agranovskaya. ZhTF **28**, 7, 1491 (1958) (in Russian).
- [5] V.A. Bokov, I.E. Myl'nikova, G.A. Smolenskii. JETP **15**, 2, 447 (1962).
- [6] G.A. Smolenskii, I.E. Chupis. Sov. Phys. Usp. **25**, 7, 475 (1982).
- [7] Z.V. Gabbasova, M.D. Kuz'min, A.K. Zvezdin, I.S. Dubenko, V.A. Murashov, D.N. Rakov, I.B. Krynetsky. Phys. Lett. A **158**, 9, 491 (1991).
- [8] W. Eerenstein, N. Mathur, J. Scott. Nature **442**, 7104, 759 (2006).
- [9] V.L. Ginzburg, A.A. Gorbatshevich, Yu.V. Kopaev, B.A. Volkov. Solid State Commun. **50**, 4, 339 (1984).
- [10] Yu.F. Popov, A.M. Kadomtseva, D.V. Belov, G.P. Vorob'ev, A.K. Zvezdin. JETP Lett. **69**, 4, 330 (1999).
- [11] Yu.F. Popov, A.M. Kadomtseva, G.P. Vorob'ev, V.A. Timofeeva, D.M. Ustinin, A.K. Zvezdin, M.M. Tegeranchi. JETP **87**, 1, 146 (1998).

- [12] B.B. Van Aken, J.P. Rivera, H. Schmid, M. Fiebig. *Nature* **449**, 7163, 702 (2007).
- [13] A.A. Gorbatshevich, O.E. Omel'yanovskii, V.I. Tsebro, A.K. Zvezdin, A.P. Pyatakov, A.A. Mukhin, V.Yu. Ivanov, V.D. Travkin, A.S. Prokhorov, A.A. Volkov, A.V. Pimenov, A.M. Shuvaev, A. Loidl, V.M. Mukhortov, Yu.I. Golovko, Yu. Yuzyuk. *Phys. Usp.* **52**, 8, 835 (2009).
- [14] Yu.V. Kopaev. *Phys. Usp.* **52**, 11, 1111 (2009).
- [15] A.A. Gorbatshevich, V.V. Kapaev, Yu.V. Kopaev. *JETP Lett.* **57**, 9, 580 (1993).
- [16] M.E. Adamova, E.A. Zhukov, A.V. Kaminskiy. *Izv. Vuzov. Priborostr.*, **62** 3, 261 (2019) (in Russian).
- [17] A.B. Ustinov, Yu.K. Fetisov, G. Srinivasan. *Tech. Phys. Lett.* **34**, 7, 593 (2008).
- [18] O.V. Antonenkov, D.A. Filippov. *Tech. Phys. Lett.* **33**, 9, 752 (2007).
- [19] A.D. Syzov, G.A. Meshkov, A.M. Monakhov, A.M. Vlasov, D.A. Sechin. *UZFF* **6**, 136302 (2013).
- [20] A. Klimov, N. Tiercelin, Y. Dusch, S. Giordano, T. Mathurin, P. Pernod, V. Preobrazhensky, A. Churbanov, S. Nikitov. *Appl. Phys. Lett.* **110**, 22, 222401 (2017).
- [21] V.D. Krevchik, E.Z. Imamov. *FTP* **17**, 7, 1235 (1983) (in Russian).
- [22] S.E. Laux, F. Stern. *Appl. Phys. Lett.* **49**, 2, 91 (1986).
- [23] C.W.J. Beenakker, H. Van Houten. In: *Solid State Physics*, v. 44 / Eds H. Ehrenreich, D. Turnbull. *Academ. Press*, New York (1991). 228 p.
- [24] T. Martin, S. Feng. *Phys. Rev. Lett.* **64**, 16, 1971 (1990).
- [25] V.D. Krevchik, A.B. Grunin, Vas.V. Evstifeev. *Semiconductors* **40**, 6, 668 (2006).
- [26] B. Mitrović, V. Milanović, Z. Ikonić. *Semicond. Sci. Technol.* **6**, 2, 93 (1991).
- [27] L. Brey, G. Platero, C. Tejedor. *Phys. Rev. B* **38**, 14, 9649 (1988).
- [28] S. Huant, S.P. Najda, B. Etienne. *Phys. Rev. Lett.* **65**, 12, 1486 (1990).
- [29] S. Huant, A. Mandray, J. Zhu, S.G. Louie, T. Pang, B. Etienne. *Phys. Rev. B* **48**, 4, 2370 (1993).
- [30] A.A. Pakhomov, K.V. Khalipov, I.N. Yassievich. *FTP* **30**, 8, 1387 (1996) (in Russian).
- [31] V.D. Krevchik, A.B. Grunin. *Phys. Solid State* **45**, 7, 1332 (2003).
- [32] A.P. Prudnikov, Yu.A. Brychkov, O.I. Marichev. *integraly i ryady*. In 3 v. V. 1. *Elementarnyye funktsii*. *Fizmatlit*, M. (2002). p. 632 (in Russian).
- [33] V.M. Verzhbitskiy. *Chislenniye metody. Matematicheskiy analiz i obyknovennyye differentsial'nyye uravneniya*. *Vyssshaya shkola*, M., (2001). 382 p. (in Russian).
- [34] I.P. Mysovskikh. *Interpolyatsionniye kubatyrniye formuly*. *Nauka*, M. (1981). p. 336 (in Russian).
- [35] D.V. Yurasov, M.N. Drozdov, A.V. Murel', A.V. Novikov. *Tech. Phys. Lett.* **37**, 9, 824 (2011).
- [36] A.P. Pyatakov, A.K. Zvezdin. *Phys. — Uspekhi* **55**, 6, 557 (2012).

*Translated by T.Zorina*